Optimization of laser-induced breakdown spectroscopy parameters from the design of experiments for multi-element qualitative analysis in river sediment

Carla Pereira de Morais[a,c,d], Gustavo Nicolodelli[b], Milene Corso Mitsuyuki[c], Stéphane Mounier[d], Débora Marcondes Bastos Pereira Milori[c,*]

[a]São Carlos Institute of Chemistry, University of São Paulo, 13566-590, São Carlos, SP, Brazil

[b]Department of Physics, Federal University of Santa Catarina, 88040-900, Florianópolis, SC, Brazil

[c]Embrapa Instrumentation, 13560-970, São Carlos, SP, Brazil

[d]University of Toulon, Aix Marseille University, CNRS/INSU, IRD, MIO UM 110, Mediterranean Institute of Oceanography, CS 60584, 83041, Toulon, Cedex 9, France.

Corresponding author

E-mail: debora.milori@embrapa.br

Phone: +55 16 2107-2801

E-mail: moraispcarla@gmail.com (Carla Pereira de Morais)

gunicolodelli@hotmail.com (Gustavo Nicolodelli)

milene.corso@embrapa.br (Milene Corso Mitsuyuki)

stephane.mounier@univ-tln.fr (Stéphane Mounier)

Abstract

Laser-induced breakdown spectroscopy (LIBS) is a fast, low analytical cost, environmentally clean technique that does not require the use of reagents for sample preparation. However, regardless of the LIBS setup, it has limitations in terms of sensitivity and precision, especially when applied to complex samples, such as river sediment. To overcome these limitations, in this work, different experimental parameters were optimized for multi-element analysis of a river sediment sample using design of experiments (DOE) approaches, i.e., fractional factorial and central composite designs (CCD). The findings demonstrated that DOE applied to the LIBS technique can be used as an efficient tool for optimizing the key parameters affecting sediment analysis by LIBS.

Keywords: LIBS, Design of experiments, Central composite design, Fractional factorial design, Sediment.

1. Introduction

Laser-induced breakdown spectroscopy (LIBS) is a fast, low analytical cost, and environmentally clean technique, which does not require the use of reagents for sample preparation [1]. However, limitations of LIBS, compared to classical analytical techniques, are lower sensitivity and precision, due to matrix effects. The sensitivity of the single pulse (SP) LIBS system can be increased using different kinds of experimental setups, such as double pulse (DP) LIBS [2,3], resonance-enhanced LIBS [4,5], microwave-assisted LIBS [6], spark discharge LIBS [7,8], spatial confinement of laser-induced plasma [9], and the use of a micro-torch [10]. In addition to instrumental techniques to improve the sensitivity of LIBS, strategies involving sample pretreatment have been used, such as the deposition of nanoparticles onto samples [11] and the addition of a salt containing easily ionizable elements [12].

In LIBS, the measurement precision is affected by matrix effects [15], the intensity of the emitted nanosecond laser, and the nonlinear interaction between the nanosecond laser and the sample matrix [15]. One of the ways to overcome this limitation is to obtain tens or hundreds of spectra distributed in different regions of the sample, to decrease the matrix effects and increase precision [16]. Some parameters that affect the plasma, such as accumulated pulses [17,18], the wavelength [19] and energy of the nanosecond lasers [20,21], and the temporal parameters (delay time and gate width) [22] play important roles in the optimization of the signal-to-noise (S/N) ratio, with their ideal values varying according to the sample composition. In DP LIBS, the inter-pulse delay is an important factor to consider for improving plasma emission [23].

Design of experiments (DOE), a methodology based on mathematical and statistical theory, is used to plan and conduct experiments by means of the analysis and interpretation of data obtained from the experiments. DOE allows input variables to be

manipulated to investigate their effects on the measured response variable [24]. When there are many factors to be optimized, it is necessary to select the variables that have the greatest effects. Fractional factorial designs can be used to perform the screening of factors [25], but since they only allow fitting of first order models, another DOE is needed to detect curvature. A three-level design (3k factorial design) is often performed to fit a second order model, but as the number of factors increases, it becomes inefficient and impractical, so a central composite design (CCD) may be used instead. CCD is a fraction of the 3k factorial design, but it does not use unnecessary degrees of freedom (which increases the cost of the experiment) [26]. The main advantage of adopting a DOE strategy, instead of testing all the different combinations of experimental parameters, consists in evidencing interactive effects among multiple parameters, reducing analysis time and costs [27]. The DOE approach has been combined with LIBS to define the most appropriate analytical parameters. For example, factorial design was used for samples of sugar cane [28] and cassava flour [29], fractional factorial design for fertilizers [30], and CCD for soils [27,31]. However, no studies have used DOE to optimize instrumental parameters in LIBS, considering SP LIBS with different lasers and the DP LIBS configuration.

The LIBS technique has been applied to investigate the elemental compositions of marine [32–34], river [35], and mining [36] sediments. However, there have been no studies concerning optimization of the key parameters affecting the analysis of complex samples such as sediments, whose matrix effects are increased by the fact that they present different characteristics in terms of texture, granulometry (contents of sand, silt, and clay), and chemical composition [37]. LIBS combined with DOE has excellent potential for applications involving sediments.

In the present work, the key parameters influencing the LIBS spectra for multi-element analysis of river sediment were optimized using CCD for SP LIBS with different wavelengths, and the combination of two DOE for DP LIBS, 2^{6-2} fractional factorial designs (one-quarter fraction) and CCD. The optimization was done to qualitatively analyze the main elements present in the river sediments. The parameters considered were laser energy, delay time, gate width, and the number of accumulated pulses. For DP LIBS, the inter-pulse delay time was also evaluated.

2. Materials and methods

2.1 Sample

One sediment sample from the Piracicaba River in Brazil (22°36'01.8" S, 48°17'53.5" W) was employed in this work to carry out all the experiments, to analyze only the effect of the instrumental variables on the response. The sample was collected using a core sampler to a depth of 15 cm in the sediment layer. The sample was freeze-dried, ground, and sieved through a 100-mesh sieve. Portions (500 mg) of the sample were compacted into pellets, using a pressure of 5 tons for 1 min.

2.2 LIBS instrumentation

The LIBS system used in this study was assembled in the laboratory, using two Nd:YAG pulsed lasers, and could operate in two different modes: (i) SP LIBS with a 1064 nm laser (Q-switched Ultra, Quantel) reaching the sample at an angle of 90°, or with a 532 nm laser (Brilliant, Quantel) reaching the sample at an angle of 45°, and (ii) DP LIBS in crossed beam configuration, combining the two different wavelength lasers, with the first pulse at 1064 nm and the second pulse at 532 nm, or with the first pulse at 532 nm and the second pulse at 1064 nm. The 1064 nm laser pulse had maximum

energy of 50 mJ, width of 8 ns, and repetition rate of 20 Hz, while the 532 nm laser pulse had maximum energy of 180 mJ, width of 4 ns, and repetition rate of 10 Hz, coupled with a second harmonic generator module. In the case of SP LIBS, a pulse delay generator (model 9618, Quantum Composers) was used for temporal control of the laser and the data acquisition system, while for DP LIBS, it was used for temporal control of the two lasers, and the data acquisition system. An echelle spectrometer (Aryelle Butterfly 400, LTB) was used to detect and select the wavelengths. The high-resolution spectrometer was equipped with an intensified charge-coupled device (ICCD) with 1024 × 1024 pixels, operated in two spectral bands (175-330 and 275-750 nm, with a resolution of 13-24 and 29-80 pm, respectively).

2.3 Spectra reproducibility

A study was carried out to evaluate how the number of spectra affects the precision of the average S/N ratio, through the simulation method consisting of the re-sampling of subsamples [38,39]. The sediment sample was analyzed by SP LIBS, and the parameters were chosen at random from the experimental runs of the CCD for SP LIBS with the 1064 nm laser. Therefore, the 1064 nm laser energy fixed at 46 mJ, the delay time at 0.5 μs, and the gate width at 5 μs. A total of 61 spectra were acquired for different regions of the pellet, with the accumulation of 9 laser pulses.

The spectra were processed using software developed in the Python programming language. After excluding outliers, using the scalar product between the average and each measured spectrum, baseline correction was performed close to each peak evaluated (Table 1) [40]. The S/N ratio for each analyte was calculated by dividing the maximum intensity of each emission line (peak height) by the standard deviation of the noise adjacent to the peak [41], resulting in 61 S/N ratios being obtained. The R

program (version 3.6.0) [42] was used to estimate the 95% confidence interval (CI) for the mean S/N ratio of the 61 spectra. Random subsets of the 61 spectra were simulated, with sizes ranging from 2 to 60 spectra. For each subset size, 1000 random samples were simulated.

Table 1. Spectroscopic atomic emission lines evaluated.

Element	Wavelength (nm)
B I	249.77
Ca I	422.67
Co I	252.13
Cr I	359.35
Cu I	324.75
Fe I	259.93
Mg I	383.82
Mn I	403.44
Na I	588.99
Ni I	232.00
P I	214.91
Sr II	407.77
V I	437.92
Zn I	213.85

For each analyte, the mean of the S/N ratio outside the 95% CI as a function of the number of spectra for each measurement is shown in Figure 1. Increase of the number of spectra leads to the average of the shot-to-shot variability of LIBS data, fewer data outside the 95% CI (above the horizontal line), consequently, increased precision of the measurement. According to the results obtained, 40-45 sample spectra

were required to ensure representativeness and increase the precision of the measurements, with the number varying from element to element.

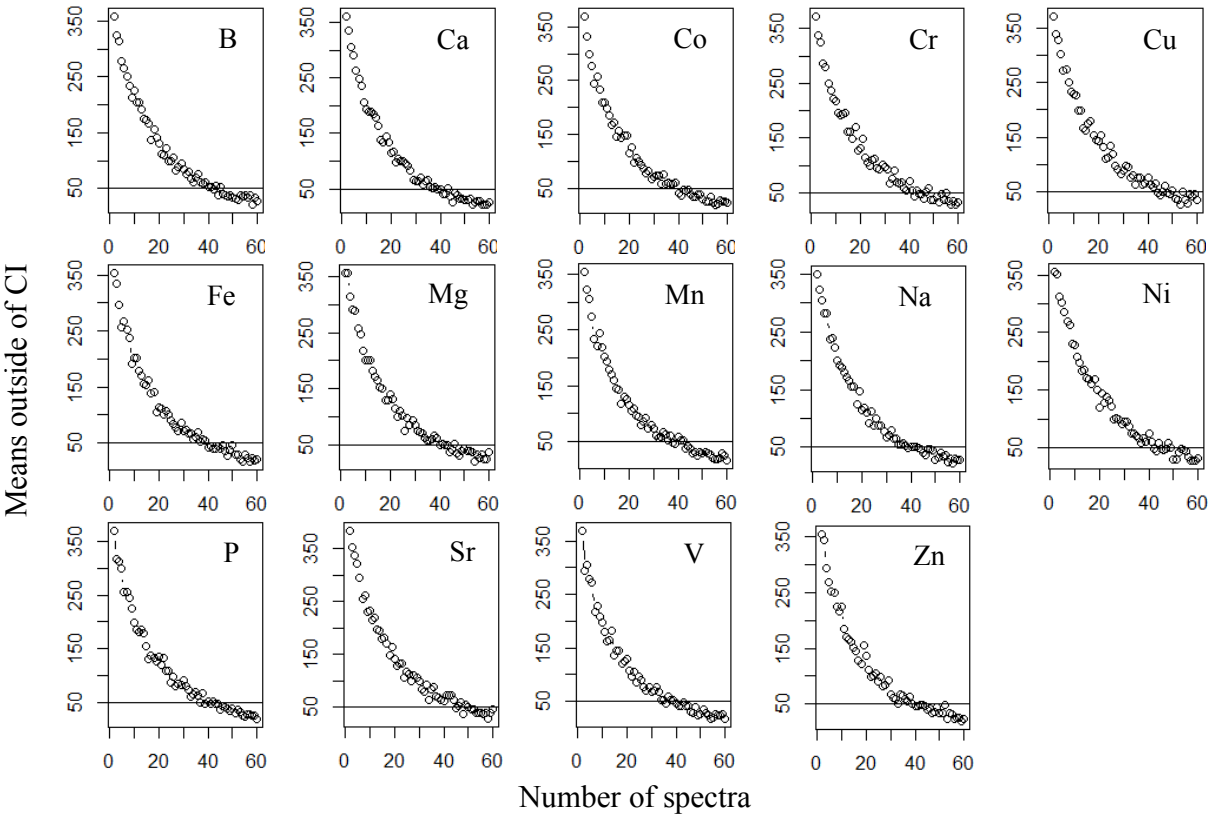

Fig. 1. Means of the S/N ratio outside the 95% CI for each analyte, as a function of the number of spectra for each measurement.

However, when the number of spectra per sample increased, the analysis time is also increased, so it is essential to establish a quantity of pulses needed to ensure the desired precision of the measurements, without losing the rapid analysis advantage of the LIBS technique. Use of this method enables determination of the number of spectra required in each measurement, bypassing the problems of lack of homogeneity of solid and complex samples, such as sediments, and plasma variables, which change from shot to shot, affecting the measurement precision [43,44]. With the aim of increasing the

precision of the measurements and overcoming the sampling problems that affect the spectral reproducibility of the LIBS analyses, while preserving the advantages of the LIBS technique in allowing rapid multi-element analysis, the number of spectra was fixed at 45 for performing all the DOE.

2.4 Design of experiments

2.4.1 Central composite design for SP LIBS with 1064 and 532 nm lasers

The central composite design (CCD) was implemented for optimization of the S/N ratio for all the elements evaluated (Table 1) in a fluvial sediment sample, with the aim of obtaining information about the linear, interaction, and quadratic effects, in order to identify a condition suitable for most of the elements. Four independent factors that influence LIBS analysis were selected for optimization: (i) laser energy (LE), (ii) delay time (DT), (iii) gate width (GW), and (iv) accumulated pulses (AP). These factors were optimized for the SP LIBS system operating with the 1064 nm laser and with the 532 nm laser.

The design had a total of $N=k^2+2k+c_p$ experimental runs, where k is the number of factors and c_p is the number of replicates at the central point. In this work, the numbers of experimental runs at factorial, axial, and central points were 16, 8, and 2, respectively, so N was 26. The CCD model was as follows [26]:

$$y=\beta_0+\sum_{i=1}^{k}\beta_i x_i+\sum_{i=1}^{k}\beta_{ii}x_i^2\sum\sum_{i<j=2}^{k}\beta_{ij}x_i x_j+\varepsilon \quad (1)$$

where, y is the response variable, β are the regression coefficients of the model, x is the independent variable, and ε is the random error component. The model errors were

assumed to be a random variable, normally and independently distributed, with zero mean and σ^2 constant variance.

The upper and lower limits for the factors were based on previous studies [2,3]. As the CCD model used was rotatable, the distance from the axial points to the central point, α, was ± 2. The values for the critical factors were calculated and studied at five levels (−α, −1, 0, +1, + α). The choice of α depends on k, and can be calculated by the following equation [26]:

$$\alpha = (2¿¿k)^{\frac{1}{4}} ¿ \quad (2)$$

For the SP LIBS system operating with the 1064 nm laser, the levels studied for each factor were as follows: (i) LE (1064 nm) = 34, 37, 40, 43, and 46 mJ; (ii) DT = 0.2, 0.5, 0.9, 1.2, and 1.5 μs; (iii) GW = 1, 5, 11, 16, and 20 μs; and (iv) AP = 1, 3, 6, 8, and 10. The same DT, GW, and AP values used in the CCD experiment for SP LIBS with the 1064 nm laser were used for SP LIBS with the 532 nm laser, with only the LE (532 nm) values being different: 35, 47, 59, 71, and 83 mJ. For each experimental run, different regions of the sediment sample pellet were used to acquire the minimum number of spectra that ensured sample representativeness.

2.4.2 Factors optimization for DP LIBS

The optimization of the S/N ratio for the same analytes studied using SP LIBS (Table 1) was performed for the fluvial sediment sample using DP LIBS, combining two DOE, because there were 6 factors to be optimized. First, two 2^{6-2} fractional factorial designs (one-quarter fraction) were implemented for DP LIBS in the crossed beam configuration, with different laser sequences (one sequence was 1064 and then 532 nm, and the other was 532 and then 1064 nm), for screening in order to discard

non-significant variables. A CCD was then performed to maximize the response using the best laser sequence.

The 2^{6-2} fractional factorial designs were performed to screen six independent factors that influenced the analysis using DP LIBS: (i) LE (1064 nm), (ii) LE (532 nm), (iii) AP, (iv) GW, (v) inter-pulse delay (ID), and (vi) DT. This design has resolution IV, so no main effects are aliased with any other, but 2-factor interactions are aliased with other 2-factor interactions. The number of experimental runs was 16, but two runs were also carried out at the central point, in order to estimate the experimental error, so the total number of runs was 18. The linear model for the fractional factorial designs was as follows [26]:

$$y = \beta_0 + \sum_{i=1}^{k} \beta_i x_i + \varepsilon \tag{3}$$

where, y is the response variable, β are the regression coefficients of the model, x is the independent variable, and ε is the random error component. The model errors were also assumed to be a random variable, normally and independently distributed, with zero mean and σ^2 constant variance.

Previous studies have been carried out to identify the maximum and minimum factor limits [2,3]. The values of the lower, intermediate, and upper levels for the factors were as follows: (i) LE (1064 nm) = 34, 40, and 46 mJ; (ii) LE (532 nm) = 35, 47, and 59 mJ; (iii) AP = 5, 18, and 10; (iv) GW = 5, 13, and 20 μs; (v) ID = 0.2, 1.6, and 3.0 μs; and (vi) DT = 0.2, 0.7, and 1.2 μs. For each experimental run, different regions of the sediment sample pellet were used to acquire the minimum number of spectra that ensured representativeness.

The 2^{6-2} fractional factorial design performed for the DP LIBS in crossed beam configuration with the best laser sequence was optimized using CCD. The three

independent factors (GW, ID, and DT) were optimized to obtain information about the linear, interaction, and quadratic effects, identifying a condition suitable for most of the elements. The number of runs was 17, including 2 runs at the central point. According to equation (2), the distance from the axial points to the central point, α, was 1.68. The values of the critical factors were calculated and varied between the upper and lower levels, as follows: GW = 5, 8, 11, 17, and 20 μs; ID = 0.2, 0.8, 1.6, 2.4, and 3.0 μs; and DT = 0.2, 0.4, 0.7, 1.0, and 1.2 μs. For each experimental run, different regions of the sediment sample pellet were used to acquire the minimum number of spectra that ensured sample representativeness.

2.4.3 Data analysis

The spectra have been analyzed as described in section 2.3. The coefficient of variation (CV) for each element was calculated for all DOE performed to assess the variability of the data and, thus, to know if the change in the values of the factors causes variation in the response. The regression models were evaluated by analysis of variance, using R software (version 3.6.0) [42]. The coefficients of determination (R^2) were calculated for the models and the relative importance (RI) for model components [45]. R^2 is a measure of the fit quality of a model, when the value of R^2 is low, it means that little of the variation in the response is attributable to its dependence on the factors. For linear models, RI provides a decomposition of the explained variation of the model into non-negative contributions, calculated based on the covariance matrix [46].

3. Results and discussion

3.1 Central composite design for SP LIBS with 1064 and 532 nm lasers

The results of the central composite design (CCD) for the SP LIBS system operating with the 1064 nm laser showed that the linear and quadratic effects of laser energy (LE) explained at most 10% of the variability for V (Table 2), with the contour graphs showing that its influence was very small (Figure 2). Hence, the lowest LE value corresponded to the optimized value. The delay time (DT) variable influenced the responses for all the elements, with the exception of Cu (Table 2), with the elements most affected being B (RI = 70%), Co (RI = 75%), and Fe (RI = 39%). For B and Co, the minimum DT value maximized the S/N ratio, while the opposite effect was observed for Fe (Figure 2). The highest coefficients of variation (CV) were found for B and Co, so the optimized DT corresponded to its lowest value. The gate width (GW) variable showed effects for 7 elements (Ca, Cr, Mg, Mn, Na, Sr, and V) (Table 2), with higher GW values resulting in maximization of the S/N ratio (Figure 2). The accumulated pulses (AP) variable showed effects for all the analytes, except Fe and Sr (Table 2). In cases where AP was significant, maximization of the S/N ratio occurred at the maximum AP value (Figure 2). The sum of the interactions between the factors represented less than 10% for all the elements, except Fe, where the LE*GW interaction represented 14%, and Zn, where DT*GW represented 21%. Therefore, the optimized factors for the SP LIBS system operating with the 1064 nm laser were LE = 34 mJ, DT = 0.2 μs, GW = 20 μs, and AP = 10.

293

294 **Table 2.** Coefficient of variation (CV), coefficient of determination (R^2), and relative
295 importance (RI) for the linear and quadratic effects in the CCD final models for SP
296 LIBS with the 1064 and 532 nm lasers.

Elements	SP LIBS 1064 nm						SP LIBS 532 nm					
	CV (%)	R^2 (%)	RI (%) of factors*				CV (%)	R^2 (%)	RI (%) of factors*			
			LE	DT	GW	AP			LE	DT	GW	AP
B	51	94		70		17	25	92	10	4		70
Ca	21	90		21	40	29	29	83		15	54	14
Co	52	94		75		11	21	82	11	9	4	45
Cr	27	93	2	15	14	54	50	80		28	45	7
Cu	17	50				50	32	69	3	9	17	8
Fe	21	57	4	39			64	89	8	58	1	19
Mg	34	91		20	10	61	43	95		8	53	31
Mn	37	94	3	4	9	75	51	87		15	45	24
Na	35	93		5	36	52	53	86		14	51	16
Ni	32	90		16		74	45	88		46	10	32
P	27	66		13		53	28	72		49	6	17
Sr	22	45	5	11	20		9	62		10	32	20
V	33	95	10	5	7	69	50	88		16	60	12
Zn	30	63		4		38	29	86	13	14		59

297 * Linear and quadratic effects.

298

299

300

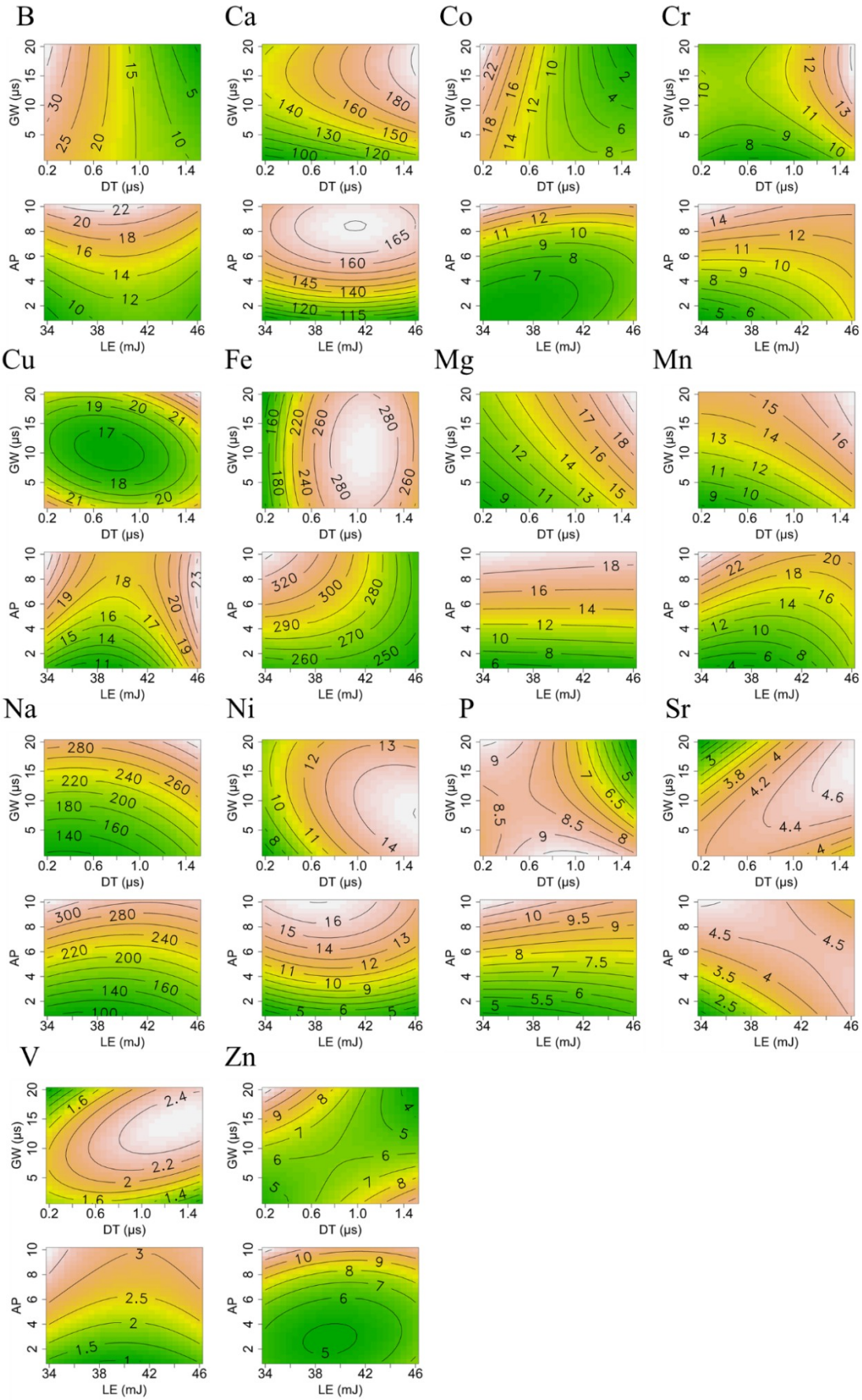

Fig. 2. S/N ratio contour graphs of the CCD model for SP LIBS with the 1064 nm laser.

For the SP LIBS system operating at 532 nm, the CCD results showed that LE only affected the responses for B, Fe, Co, and Zn, with RI of 10, 11, 8, and 13%, respectively (Table 2). Among these elements, Fe presented the highest CV of 64%, corresponding to the greatest effect of LE. Since the lowest LE value maximized the S/N ratio for Fe (Figure 3), while for the other elements LE had little or no effect, the lowest value of LE was adopted as the optimum. An effect of DT was observed for all the elements (Table 2). Since the lowest value was only indicated for B and Co (Figure 3), the highest value of DT was adopted as optimal. Among the elements whose response was affected by GW (Table 2), all showed the highest response at the maximum value, with the exception of Cr (Figure 3). All the elements showed an effect of AP (Table 2), with the highest response at the maximum value, with the exception of Fe (Figure 3). The sum of the interactions between the factors represented less than 10% for all elements, except for Co, where the LE*DT and GW*AP interactions both represented 6.5%, and for Cu, where the LE*GW, LE*AP, and GW*AP interactions represented 14, 8, and 10%, respectively. For the SP LIBS system operating at 532 nm (Table 2 and Figure 3), the optimized factors were LE = 35 mJ, DT = 1.5 μs, GW = 20 μs, and AP = 10.

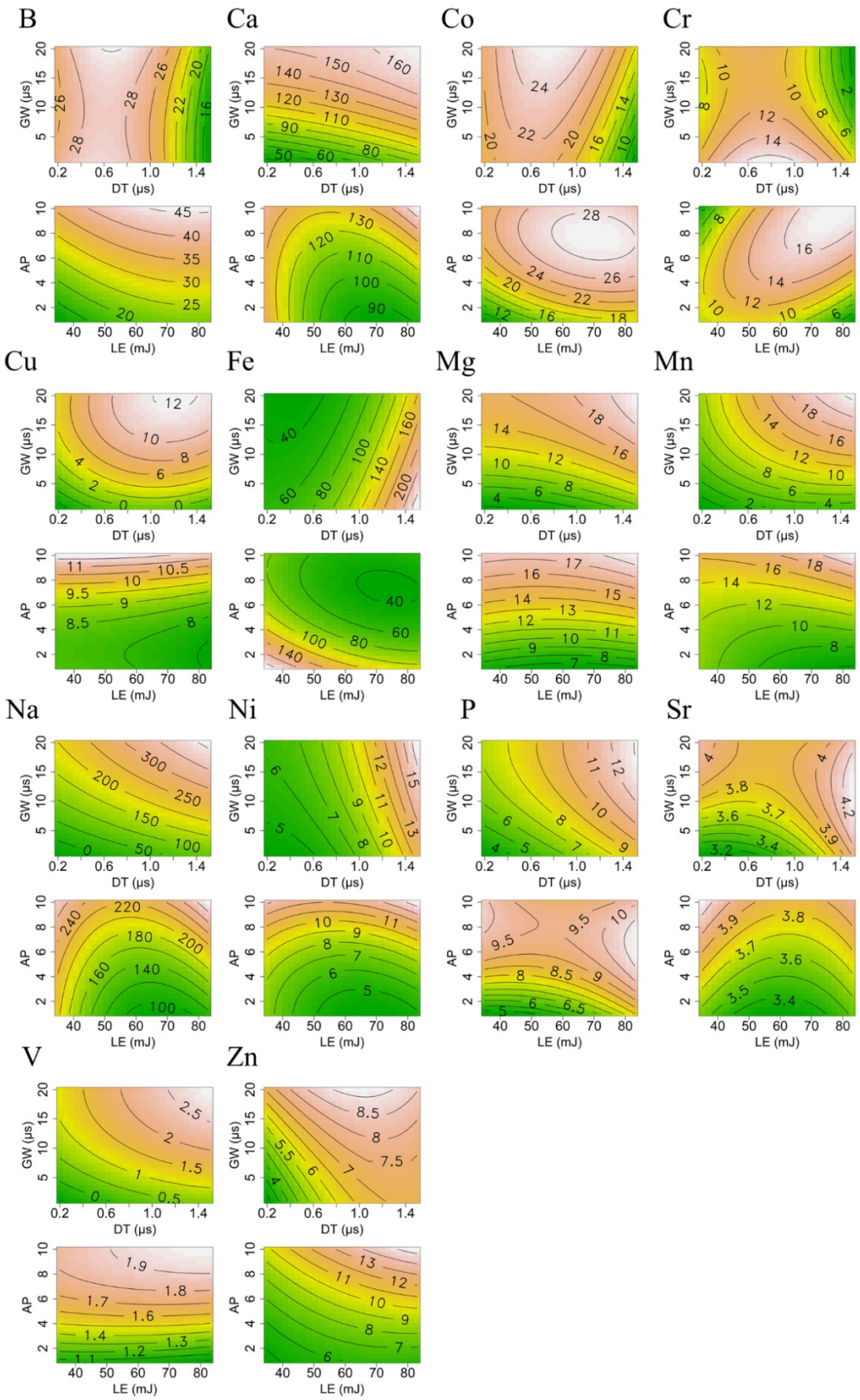

Fig. 3. S/N ratio contour graphs of the CCD model for SP LIBS with the 532 nm laser.

The optimization of the factors that influenced the multi-element analysis of sediment by SP LIBS (1064 and 532 nm lasers) showed that in cases where the CV was less than 10%, the response variation in all the runs did not have a significant effect, regardless of the combination of values studied for each factor. In LIBS, the breakdown events dramatically change the spectral line intensities, consequently increasing the CV of the measurements. For geochemical analyses, CV values between 5 and 20% are generally acceptable [16]. The RI of the factors studied for each element helped to identify the most important variables from the percentage contributions.

For both SP LIBS systems, the lowest LE value was chosen as the optimum, because LE in the studied range had little or no influence on the S/N ratio of the elements evaluated. Studies have shown that the intensities of the emission lines of the LIBS spectrum increase with the laser energy, under constant irradiance [47,48]. However, increasing the intensity of the emission lines can lead to increased noise, so it is important to evaluate the S/N ratio [41].

For both SP LIBS systems, the highest GW and AP values maximized the S/N ratio. However, for the 1064 nm laser, the lowest DT value maximized the S/N ratio for most elements, while for the 532 nm laser the highest value of this factor maximized the response for most elements. These results were related to the mechanisms of plasma generation and formation. The cascade-like growth of the electron density (inverse bremsstrahlung) is more favorable for longer wavelength lasers [49], while multiphoton ionization plays an important role for short wavelength lasers [21].

3.2 Factors optimization for DP LIBS

Two 2^{6-2} fractional factorial designs were implemented for DP LIBS with different laser sequences (one sequence was 1064-532 nm, and the other was 532-1064

nm), for choosing the best laser sequence and screening to discard non-significant variables. The 2^{6-2} fractional factorial design with the 1064-532 nm laser sequence (Table 3) showed that the 1064 nm LE had no influence on the S/N ratio, for any element, while the 532 nm LE explained at most 10% of the variability (for Fe). The other factors had greater effects on the S/N ratio, with effects ≤43% for AP (10 elements: B, Ca, Co, Cr, Mg, Mn, Na, P, V, and Zn), ≤29% for GW (4 elements: Cr, Mg, Mn, and Na), ≤66% for inter-pulse delay (ID) (6 elements: B, Co, Mg, Ni, P, and Zn), and ≤58% for DT (10 elements: B, Co, Cu, Fe, Mg, Mn, Ni, P, Sr, and Zn). The 2^{6-2} fractional factorial design with the 532-1064 nm laser sequence (Table 3) again showed that the 1064 nm LE had no influence on the S/N ratio for any element, while the 532 nm LE explained at most 20% of the variability (for Zn). The other factors had greater influence on the S/N ratio, with effects ≤42% for AP (11 elements: B, Ca, Co, Cu, Cr, Mg, Mn, Ni, P, V, and Zn), ≤41% for GW (4 elements: Cr, Mg, Mn, and Sr), ≤85% for ID (6 elements: B, Ca, Co, Fe, Mg, and Na), and ≤43% for DT (10 elements: B, Ca, Co, Cr, Mg, Na, Ni, P, V, and Zn).

Elements	2^{6-2} fractional factorial design with the 1064-532 nm laser sequence								2^{6-2} fractional factorial design with the 532-1064 nm laser sequence							
	CV (%)	R^2 (%)	RI (%) of factors*						CV (%)	R^2 (%)	RI (%) of factors*					
			1064 nm LE	532 nm LE	AP	GW	ID	DT			1064 nm LE	532 nm LE	AP	GW	ID	DT
B	52	85		5	7		16	57	59	76			15		18	43
Ca	50	43			43				39	96			2		85	9
Co	64	90		3	8		24	55	62	82		8	15		16	43
Cu	27	42						42	28	28			28			
Cr	30	47			18	29			24	60			20	18		22
Fe	47	66		10				56	48	32					32	
Mg	37	76			34	12	23	7	23	74			37	12	14	11
Mn	40	58			26	19		13	26	58			42	16		
Na	65	68			43	25			29	51					29	22
Ni	42	74					66	8	38	53		14	16			23
P	43	74			8		47	19	47	35			19			16
Sr	39	58						58	7	41				41		
V	27	18			18				10	41			15			26
Zn	52	88		9	18		46	15	41	63		20	13			30

*Linear effect.

Table 3. Coefficient of variation (CV), coefficient of determination (R^2), and relative importance (RI) for linear effects in the fractional factorial design final models for DP LIBS.

The 2^{6-2} fractional factorial design with the 532-1064 nm laser sequence showed better performance (higher S/N ratios), compared to the 1064-532 nm laser sequence. This was expected, because the background emission was higher when the 1064 nm laser was used for sample ablation [2]. Hence, the 2^{6-2} fractional factorial design with the 532-1064 nm laser sequence, where the 1064 nm laser was used to reheat the plasma, was optimized using a CCD.

According to the results obtained by 2^{6-2} fractional factorial design with the 532-1064 nm laser sequence, the values of the factors that were fixed were chosen, and then the factors that had the greatest effects on the S/N ratio were optimized through the CCD. The results showed that for the 2^{6-2} fractional factorial design with the 532-1064 nm laser sequence, the LE for the 1064 nm laser did not influence the S/N ratio for any element, while the LE for the 532 nm pulse explained very little of the data variability. Therefore, these two factors were fixed at their lowest values (34 and 35 mJ for the 1064 and 532 nm lasers, respectively) for implementation of the CCD. Higher values of AP resulted in maximization of the S/N ratio for all the elements influenced by this factor (with the exception of Ca, for which the RI value was only 2%). In addition, it was observed that for the SP LIBS system operating with the 1064 and 532 nm lasers, the highest S/N ratio also occurred at the maximum AP value. Therefore, this factor was fixed at its highest value (10 accumulated pulses) for implementation of the CCD. Since the factors GW, ID, and DT had the greatest effects on the S/N ratio, they were selected for refining the optimal conditions.

In the CCD experiment, Sr presented little variation of the S/N ratio, with CV of only 2% (Table 4). Consequently, no factor affected the response of this element. GW only affected the S/N ratio for Cr and Zn (Table 4), both with RI of 9%, so the lowest value of this factor corresponded to its optimized value. ID influenced 13 elements

(Table 4), most of which showed a maximum response at the minimum ID value, except Ca, Fe, and Mg, for which the intermediate value represented the best condition (Figure 4). DT affected 8 elements (Table 4), of which 5 elements (N, Co, Ni, P, and Zn) presented a maximum response at the minimum DT value (Figure 4). For Ca and Mg, the best condition was at the maximum DT value, while for Fe it was at an intermediate value. However, the CV values for Ca and Fe were below 15%. The sum of the interactions between the factors corresponded to less than 10% for most elements, except B and Fe, for which the ID*DT interaction corresponded to 2 and 16%, respectively. Therefore, the optimized factors for DP LIBS in crossed beam configuration with the 532-1064 nm laser sequence were as follows: LE (1064 nm) = 34 mJ; LE (532 nm) = 35 mJ; AP = 10; GW = 5 μs; ID = 0.2 μs; and DT = 0.2 μs.

Table 4. Coefficient of variation (CV), coefficient of determination (R^2), and relative importance (RI) for the linear and quadratic effects in the CCD final models for DP LIBS.

Element	CV (%)	R^2 (%)	RI (%) of factors*		
			GW	ID	DT
B	97	99		72	25
Ca	14	95		73	22
Co	113	92		81	11
Cu	16	67		67	
Cr	14	72	9	63	
Fe	14	72		42	14
Mg	22	83		54	29
Mn	23	80		80	
Na	13	42		42	
Ni	108	92		72	20
P	67	99		69	30
Sr	2				
V	16	83		83	
Zn	56	57	9	15	33

* Linear and quadratic effects.

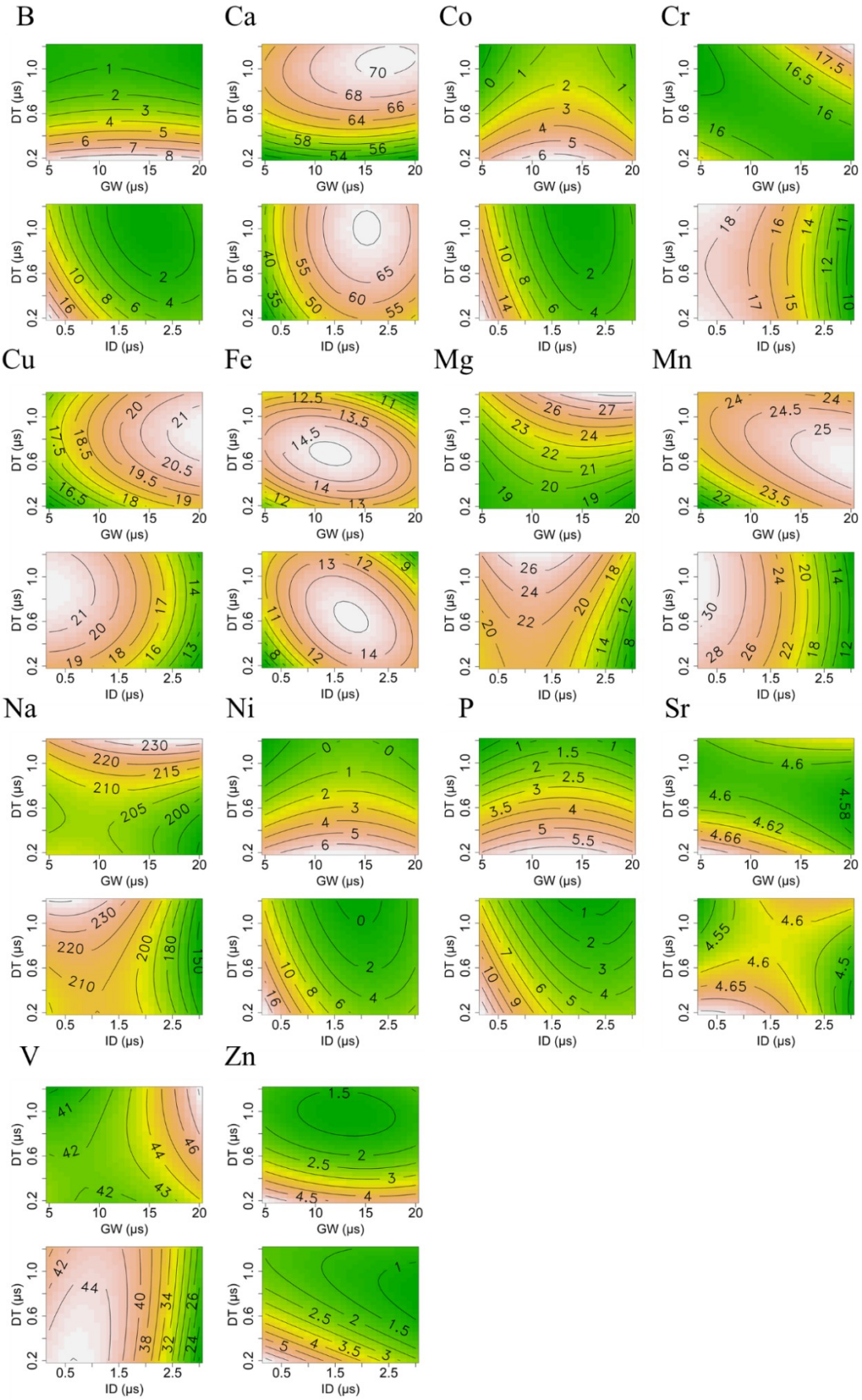

Fig. 4. S/N ratio contour graphs of the CCD model for DP LIBS.

As in the case of SP LIBS, LE in the range studied had little or no influence on the S/N ratio for the elements evaluated, while the highest AP value maximized the S/N ratio. Different to SP LIBS, the lowest GW value maximized the response. The optimized DT for DP LIBS was the same as that for SP LIBS with the 1064 nm laser (0.2 μs). The maximization of the S/N ratio at the lowest DT value was due to the higher excitation temperature and electron density at the beginning of plasma formation [2]. For the elements influenced by ID, most presented a maximum response at ID of 0.2 μs, because the plasma absorbed the energy from the 1064 nm laser that reheated the plasma (second pulse), consequently increasing the temperature of the plasma formed by the 532 nm laser [50].

4. Conclusions

The parameters that influence the qualitative multi-elemental analysis of a sediment sample from the Piracicaba River by SP LIBS (1064 nm and 532 nm lasers) were optimized using a central composite design (CCD) for each system, preserving the multi-element advantage of this technique. In the data range evaluated, the laser energy (LE) had little or no influence on the S/N ratio for the elements studied, using both SP LIBS. Regardless of the system, the maximum accumulated pulses (AP) and gate width (GW) values maximized the responses for most of the elements affected by these factors. However, for SP LIBS at 1064 nm laser, the use of the delay time (DT) at its lowest value maximized the S/N ratio for most elements, while for SP LIBS at 532 nm, the highest value of this factor maximized the response for most elements.

The 2^{6-2} fractional factorial design for DP LIBS showed that the 532-1064 nm laser sequence provided the best performance, so this system was optimized using a CCD. According to the results obtained by 26-2 fractional factorial design with the 532-

1064 nm laser sequence, the factors GW, ID, and DT had the greatest effects on the S/N ratio, they were selected for refining the optimal conditions. Unlike SP LIBS, the response was maximized at the lowest GW value. The optimized DT for DP LIBS was the same as for SP LIBS with the 1064 nm laser. For the elements affected by ID, most presented a maximum response at the lowest ID value.

The DOE allowed describing the combined effects of the factors in the response using a smaller number of experiments and then saving time and costs, when compared to the optimization of a factor at a time. The CCD combined with the LIBS technique proved to be an excellent tool for optimizing the parameters that affect the LIBS analysis, and the fractional factorial design proved to be very efficient for screening and deciding which factors deserve further study.

Acknowledgements

This study was financed in part by the Coordenação de Aperfeiçoamento de Pessoal de Nível Superior - Brasil (CAPES) Finance Code 001, grant number - 88882.331025/2019-01 for providing a fellowship to Carla Pereira de Morais, FAPESP grant numbers (2013/07276-1 and 16/14227-5), CNPq grant number (403405/2013-0), and EMBRAPA Instrumentation.

References

[1] C. Pasquini, J. Corttez, L.M.C. Silva, F.B. Gonzaga, Laser-induced breakdown spectroscopy, J. Brazilian Chem. Soc. 18 (2007) 463. https://doi.org/10.1366/000370210793561691.

[2] G. Nicolodelli, G.S. Senesi, R.A. Romano, I.L. De Oliveira Perazzoli, D.M.B.P. Milori, Signal enhancement in collinear double-pulse laser-induced breakdown

spectroscopy applied to different soils, Spectrochim. Acta Part B At. Spectrosc. 111 (2015) 23–29. https://doi.org/10.1016/j.sab.2015.06.008.

[3] G. Nicolodelli, G.S. Senesi, A.C. Ranulfi, B.S. Marangoni, A. Watanabe, V. de Melo Benites, P.P.A. de Oliveira, P. Villas-Boas, D.M.B.P. Milori, Double-pulse laser induced breakdown spectroscopy in orthogonal beam geometry to enhance line emission intensity from agricultural samples, Microchem. J. 133 (2017) 272–278. https://doi.org/10.1016/j.microc.2017.03.047.

[4] C. Goueguel, S. Laville, F. Vidal, M. Sabsabi, M. Chaker, Investigation of resonance-enhanced laser-induced breakdown spectroscopy for analysis of aluminium alloys, J. Anal. At. Spectrom. 25 (2010) 635–644. https://doi.org/10.1039/b927013b.

[5] G. Nicolodelli, P.R. Villas-Boas, C.R. Menegatti, G.S. Senesi, D. V. Magalhães, D. de Souza, D.M.B.P. Milori, B.S. Marangoni, Determination of Pb in soils by double-pulse laser-induced breakdown spectroscopy assisted by continuum wave-diode laser-induced fluorescence, Appl. Opt. 57 (2018) 8366. https://doi.org/10.1364/ao.57.008366.

[6] Y. Liu, M. Baudelet, M. Richardson, Elemental analysis by microwave-assisted laser-induced breakdown spectroscopy: Evaluation on ceramics, J. Anal. At. Spectrom. 25 (2010) 1316–1323. https://doi.org/10.1039/c003304a.

[7] O.A. Nassef, H.E. Elsayed-Ali, Spark discharge assisted laser induced breakdown spectroscopy, Spectrochim. Acta - Part B At. Spectrosc. 60 (2005) 1564–1572. https://doi.org/10.1016/j.sab.2005.10.010.

[8] A. Lima, T. Varão, F. Schiavon, I. De Sousa, G. Saverio, D. Santos, E. Cristina, J. Anchieta, G. Neto, Determinations of phosphorus in fertilizers by spark discharge-assisted laser-induced breakdown spectroscopy, Microchem. J. 139

(2018) 322–326. https://doi.org/https://doi.org/10.1016/j.microc.2018.03.011.

[9] A.M. Popov, F. Colao, R. Fantoni, Spatial confinement of laser-induced plasma to enhance LIBS sensitivity for trace elements determination in soils, J. Anal. At. Spectrom. 25 (2010) 837. https://doi.org/10.1039/b919485a.

[10] L. Liu, X. Huang, S. Li, Y. Lu, K. Chen, L. Jiang, J.F. Silvain, Y.F. Lu, Laser-induced breakdown spectroscopy enhanced by a micro torch, Opt. Express. 23 (2015) 15047. https://doi.org/10.1364/oe.23.015047.

[11] A. De Giacomo, R. Gaudiuso, C. Koral, M. Dell'Aglio, O. De Pascale, Nanoparticle-enhanced laser-induced breakdown spectroscopy of metallic samples, Anal. Chem. 85 (2013) 10180–10187. https://doi.org/10.1021/ac4016165.

[12] C.P. de Morais, A.I. Barros, M.A. Bechlin, T.V. Silva, D.S. Júnior, G.S. Senesi, M.S. Crespi, C.A. Ribeiro, J.A. Gomes Neto, E.C. Ferreira, Laser-induced breakdown spectroscopy determination of K in biochar-based fertilizers in the presence of easily ionizable element, Talanta. 188 (2018) 199–202. https://doi.org/10.1016/j.talanta.2018.05.089.

[13] D.A. Cremers, L.J. Radziemski, Handbook of Laser-Induced Breakdown Spectroscopy, John Wiley & Sons, U.K., 2013.

[14] S.N. Singh, J.P., Thakur, Laser Induced Breakdown spectroscopy, Elsevier B.V, Amsterdam, 2007.

[15] R. NOLL, Laser-Induced Breakdown Spectroscopy - fundamentals and applications, Springer-Verlag, Heidelberg, 2012.

[16] U. Perini, S. Musazzi, eds., Laser-Induced Breakdown Spectroscopy: Theory and Applications, Springer-Verlag Berlin Heidelberg, Heidelberg, 2014.

[17] B.C. Castle, K. Talabardon, B.W. Smith, J.D. Winefordner, Variables influencing

the precision of laser-induced breakdown spectroscopy measurements, Appl. Spectrosc. 52 (1998) 649–657. https://doi.org/10.1366/0003702981944300.

[18] M.A. Gondal, T. Hussain, Z.H. Yamani, M.A. Baig, The role of various binding materials for trace elemental analysis of powder samples using laser-induced breakdown spectroscopy, Talanta. 72 (2007) 642–649. https://doi.org/10.1016/j.talanta.2006.11.039.

[19] D.W. Hahn, N. Omenetto, Laser-induced breakdown spectroscopy (LIBS), part I: Review of basic diagnostics and plasmaparticle interactions: Still-challenging issues within the analytical plasma community, Appl. Spectrosc. 64 (2010). https://doi.org/10.1366/000370210793561691.

[20] J.M. Vadillo, J.M. Fernández Romero, C. Rodríguez, J.J. Laserna, Effect of plasma shielding on laser ablation rate of pure metals at reduced pressure, Surf. Interface Anal. 27 (1999) 1009–1015. https://doi.org/10.1002/(SICI)1096-9918(199911)27:11<1009::AID-SIA670>3.0.CO;2-2.

[21] J.P. Singh, S.N. Thankur, Laser-Induced Breakdown Spectroscopy, Elsevier Science, Amsterdam, 2007.

[22] A. Ciucci, V. Palleschi, S. Rastelli, R. Barbini, F. Colao, R. Fantoni, A. Palucci, S. Ribezzo, H.J.L. Van Der Steen, Trace pollutants analysis in soil by a time-resolved laser-induced breakdown spectroscopy technique, Appl. Phys. B Lasers Opt. 63 (1996) 185–190. https://doi.org/10.1007/BF01095271.

[23] S. Nakamura, Y. Ito, K. Sone, H. Hiraga, K.I. Kaneko, Determination of an Iron Suspension in Water by Laser-Induced Breakdown Spectroscopy with Two Sequential Laser Pulses, Anal. Chem. 68 (1996) 2981–2986. https://doi.org/10.1021/ac9601167.

[24] B. Durakovic, Design of experiments application, concepts, examples: State of

the art, Period. Eng. Nat. Sci. 5 (2017) 421–439. https://doi.org/10.21533/pen.v5i3.145.

[25] A.C. Atkinson, A.N. Donev, R.D. Tobias, Optimum Experimental Designs, with SAS, Oxford University Press, 2007.

[26] R.L. Mason, R.F. Gunst, J.L. Hess, Statistical Design and Analysis of Experiments: With Applications to Engineering and Science, Second Edition., John Wiley & Sons, 2003.

[27] K. Yu, Y. Zhao, Y. He, D. He, Response surface methodology for optimizing LIBS testing parameters: A case to conduct the elemental contents analysis in soil, Chemom. Intell. Lab. Syst. 195 (2019) 103891. https://doi.org/10.1016/j.chemolab.2019.103891.

[28] J.P.R. Romera, P.L. Barsanelli, F.M.V. Pereira, Expeditious prediction of fiber content in sugar cane: An analytical possibility with LIBS and chemometrics, Fuel. 166 (2016) 473–476. https://doi.org/10.1016/j.fuel.2015.11.029.

[29] V.C. Costa, D.V. de Babos, F.W.B. de Aquino, A. Virgílio, F.A.C. Amorim, E.R. Pereira-Filho, Direct Determination of Ca, K and Mg in Cassava Flour Samples by Laser-Induced Breakdown Spectroscopy (LIBS), Food Anal. Methods. 11 (2018) 1886–1896. https://doi.org/10.1007/s12161-017-1086-9.

[30] D.F. Andrade, E.R. Pereira-Filho, Direct Determination of Contaminants and Major and Minor Nutrients in Solid Fertilizers Using Laser-Induced Breakdown Spectroscopy (LIBS), J. Agric. Food Chem. 64 (2016) 7890–7898. https://doi.org/10.1021/acs.jafc.6b04028.

[31] V.C. Costa, S. dos Santos Ferreira, L.N. Santos, M.A. Sperança, C.S. da Silva, G.A. Sodré, E.R. Pereira-Filho, Qualitative and Quantitative Analysis of Soils Using Laser-Induced Breakdown Spectroscopy and Chemometrics Tools, J.

Appl. Spectrosc. 87 (2020) 378–386. https://doi.org/10.1007/s10812-020-01010-5.

[32] R. Barbini, F. Colao, V. Lazic, R. Fantoni, A. Palucci, M. Angelone, On board LIBS analysis of marine sediments collected during the XVI Italian campaign in Antarctica, Spectrochim. Acta Part B At. Spectrosc. 57 (2002) 1203–1218. https://doi.org/10.1016/S0584-8547(02)00055-1.

[33] V. Lazic, R. Barbini, F. Colao, R. Fantoni, A. Palucci, Self-absorption model in quantitative laser induced breakdown spectroscopy measurements on soils and sediments, Spectrochim. Acta Part B At. Spectrosc. 56 (2001) 807–820. https://doi.org/10.1016/S0584-8547(01)00211-7.

[34] V. Lazic, F. Colao, R. Fantoni, V. Spizzichino, S. Jovićević, Underwater sediment analyses by laser induced breakdown spectroscopy and calibration procedure for fluctuating plasma parameters, Spectrochim. Acta Part B At. Spectrosc. 62 (2007) 30–39. https://doi.org/10.1016/j.sab.2006.11.004.

[35] E.S. Austria, E.M. Fuentes, G.M. Nuesca, R.B. Lamorena, Laser-induced breakdown spectroscopy for the quantitative analysis of metals in sediments using natural zeolite matrix, Spectrochim. Acta Part B At. Spectrosc. 136 (2017) 1–7. https://doi.org/10.1016/j.sab.2017.07.001.

[36] E.S. Austria, G.M. Nuesca, R.B. Lamorena, Spectral fitting approach for the determination of enrichment and contamination factors in mining sediments using laser-induced breakdown spectroscopy, Environ. Sci. Pollut. Res. 25 (2018) 16620–16628. https://doi.org/10.1007/s11356-018-1803-y.

[37] D. Han, Y.J. Joe, J.S. Ryu, T. Unno, G. Kim, M. Yamamoto, K. Park, H.G. Hur, J.H. Lee, S. Il Nam, Application of laser-induced breakdown spectroscopy to Arctic sediments in the Chukchi Sea, Spectrochim. Acta - Part B At. Spectrosc.

146 (2018) 84–92. https://doi.org/10.1016/j.sab.2018.05.002.

[38] M.S. de O. Leite, L.A. Peternelli, M.H.P. Barbosa, P.R. Cecon, C.D. Cruz, Sample size for full-sib family evaluation in sugarcane, Pesqui. Agropecuária Bras. 44 (2009) 1562–1574. https://doi.org/10.1590/s0100-204x2009001200002.

[39] A.R. da Silva, E.R. do Rêgo, P.R. Cecon, Tamanho de amostra para caracterização morfológica de frutos de pimenteira, Hortic. Bras. 29 (2011) 125–129. https://doi.org/10.1590/S0102-05362011000100022.

[40] B.S. Marangoni, K.S.G. Silva, G. Nicolodelli, G.S. Senesi, J.S. Cabral, P.R. Villas-Boas, C.S. Silva, P.C. Teixeira, A.R.A. Nogueira, V.M. Benites, D.M.B.P. Milori, Phosphorus quantification in fertilizers using laser induced breakdown spectroscopy (LIBS): A methodology of analysis to correct physical matrix effects, Anal. Methods. 8 (2016) 78–82. https://doi.org/10.1039/c5ay01615k.

[41] D.W. Hahn, N. Omenetto, Laser-induced breakdown spectroscopy (LIBS), part II: Review of instrumental and methodological approaches to material analysis and applications to different fields, Appl. Spectrosc. 66 (2012) 347–419. https://doi.org/10.1366/11-06574.

[42] R Core Team (2018). R: A language and environmente for statistical computing. R Foundation for Statistical Computing, Vienna, Austria., (n.d.). http://www.r-project.org/.

[43] A.W. Miziolek, V. Palleschi, I. Schechter, Laser Induced Breakdown Spectroscopy (LIBS): Fundamentals and Applications, Cambridge University Press, New York, 2006.

[44] J.R. Wachter, D.A. Cremers, Determination of Uranium in Solution Using Laser-Induced Breakdown Spectroscopy., Appl. Spectrosc. 41 (1987) 1042–1048. https://doi.org/10.1366/0003702874447897.

[45] Groemping, U. (2006) Relative Importance for Linear Regression in R: The Package relaimpo Journal of Statistical Software 17, Issue 1. Downloadable at http://www.jstatsoft.org/v17/i01, (n.d.).

[46] R.H. Lindeman, P.F. Merenda, R.Z. Gold, Introduction to Bivariate and Multivariate Analysis, Scott Foresman & Co, Glenview, IL, 1980.

[47] J.A. Aguilera, C. Aragón, Characterization of laser-induced plasmas by emission spectroscopy with curve-of-growth measurements. Part II: Effect of the focusing distance and the pulse energy, Spectrochim. Acta - Part B At. Spectrosc. 63 (2008) 793–799. https://doi.org/10.1016/j.sab.2008.04.013.

[48] G.G.A. De Carvalho, D. Santos, L.C. Nunes, M.D.S. Gomes, F.D.O. Leme, F.J. Krug, Effects of laser focusing and fluence on the analysis of pellets of plant materials by laser-induced breakdown spectroscopy, Spectrochim. Acta - Part B At. Spectrosc. 74–75 (2012) 162–168. https://doi.org/10.1016/j.sab.2012.06.012.

[49] L.M. Cabalin, J.J. Laserna, Experimental determination of laser induced breakdown thresholds of metals under nanosecond Q-switched laser operation, Spectrochim. Acta, Part B At. Spectrosc. 53 (1998) 723–730. https://doi.org/10.1016/S0584-8547(98)00107-4.

[50] C. Gautier, P. Fichet, D. Menut, J.L. Lacour, D. L'Hermite, J. Dubessy, Quantification of the intensity enhancements for the double-pulse laser-induced breakdown spectroscopy in the orthogonal beam geometry, Spectrochim. Acta - Part B At. Spectrosc. 60 (2005) 265–276. https://doi.org/10.1016/j.sab.2005.01.006.